catalysts

MDPI

Supplemental information

Interface Engineering of SRu-mC$_3$N$_4$ Heterostructures for Enhanced Electrochemical Hydrazine Oxidation Reactions

Ajay Munde [1,†], Priti Sharma [2,†], Somnath Dhawale [1], Ravishankar G. Kadam [2], Subodh Kumar [3], Hanumant B. Kale [4], Jan Filip [2], Radek Zboril [2,5], Bhaskar R. Sathe [1,*] and Manoj B. Gawande [2,4,*]

[1] Department of Chemistry, Dr. Babasaheb Ambedkar Marathwada University, Aurangabad 431004, Maharashtra, India
[2] Regional Centre of Advanced Technologies and Materials, Czech Advanced Technology and Research Institute, Palacký University, Šlechtitelů 27, 779 00 Olomouc, Czech Republic
[3] Department of Inorganic Chemistry, Faculty of Science, Palacký University, 17. Listopadu 12, 771 46 Olomouc, Czech Republic
[4] Department of Industrial and Engineering Chemistry, Institute of Chemical Technology, Mumbai-Marathwada Campus, Jalna 431213, Maharashtra, India
[5] CEET, Nanotechnology Centre, VŠB–Technical University of Ostrava, 17. Listopadu 2172/15, 708 00 Ostrava, Czech Republic
* Correspondence: bsathe.chemistry@bamu.ac.in (B.R.S.); mb.gawande@marj.ictmumbai.edu.in (M.B.G.)
† These authors contributed equally to this work.

Supplemental information list

S-1) Synthesis methods

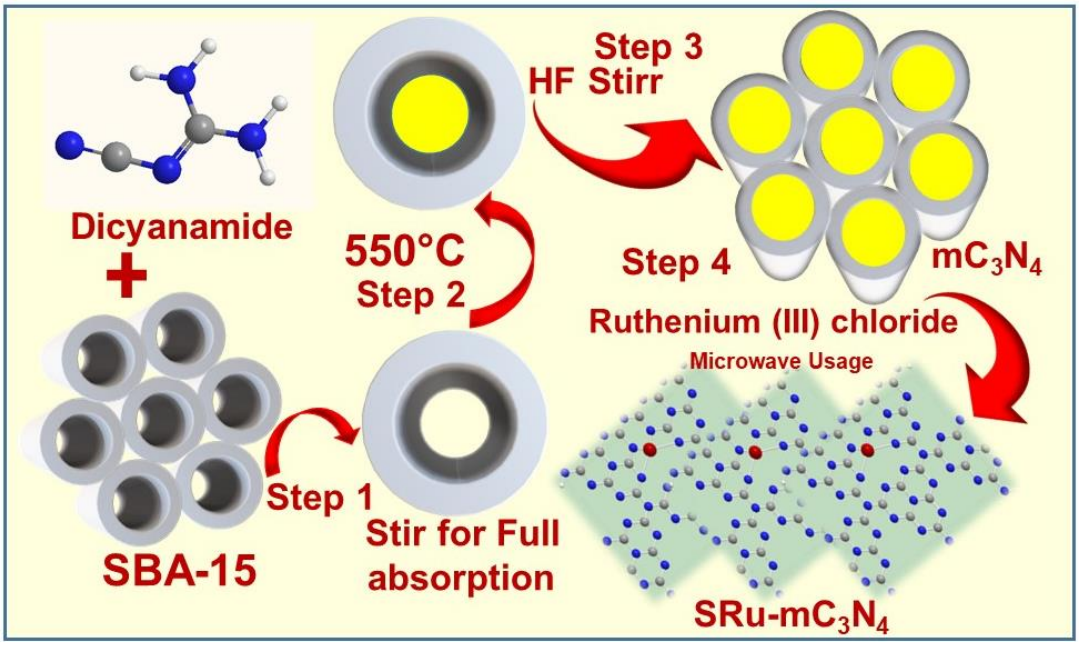

Scheme S1. Schematic representation for protocol depicting formulation of ruthenium single atom over mesoporous C_3N_4 ($SRu\text{-}mC_3N_4$).

S-2) Wide-angle XRD pattern

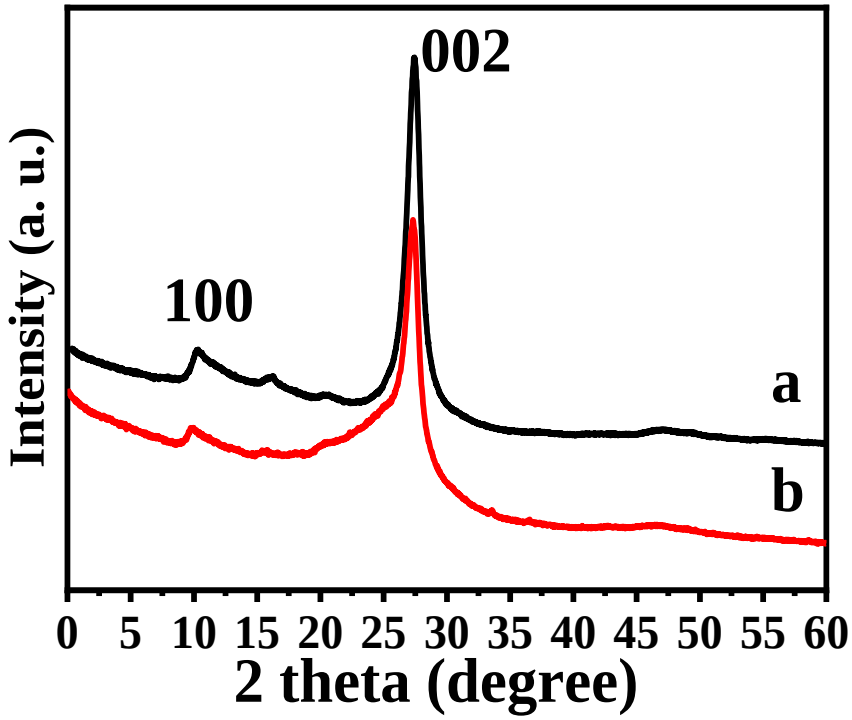

Figure S1. Wide-angle XRD pattern of $SRu\text{-}mC_3N_4$; a) mC_3N_4; and b) $SRu\text{-}mC_3N_4$.

S-3) High-resolution XPS spectra

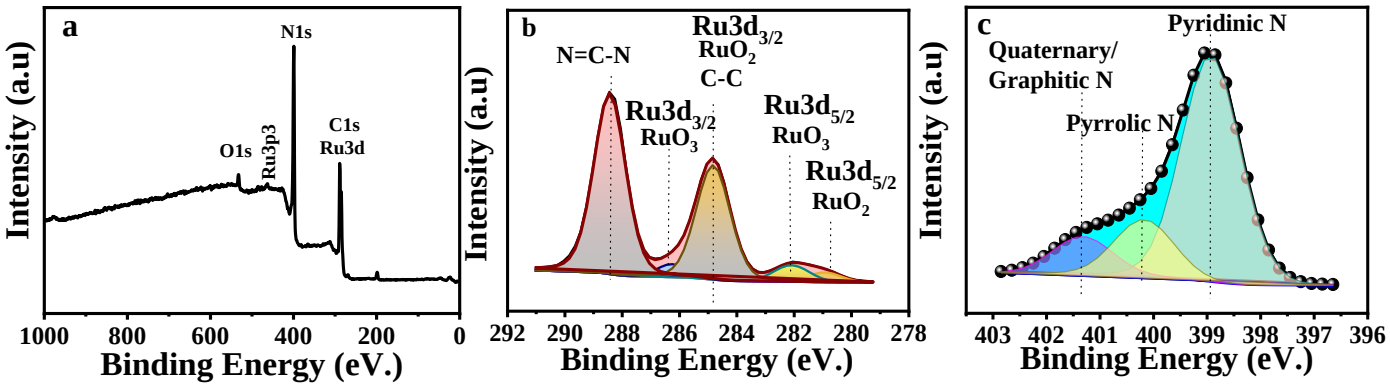

Figure S2. High-resolution XPS spectra of SRu-mC$_3$N$_4$: a) Full scan; b) N1s spectra of SRu-mC$_3$N$_4$; c) Ru 3d High-resolution XPS spectra of SRu-mC$_3$N$_4$ with carbon.

S-4) Electrochemical Studies

i) Linear sweep voltammetry (LSV)

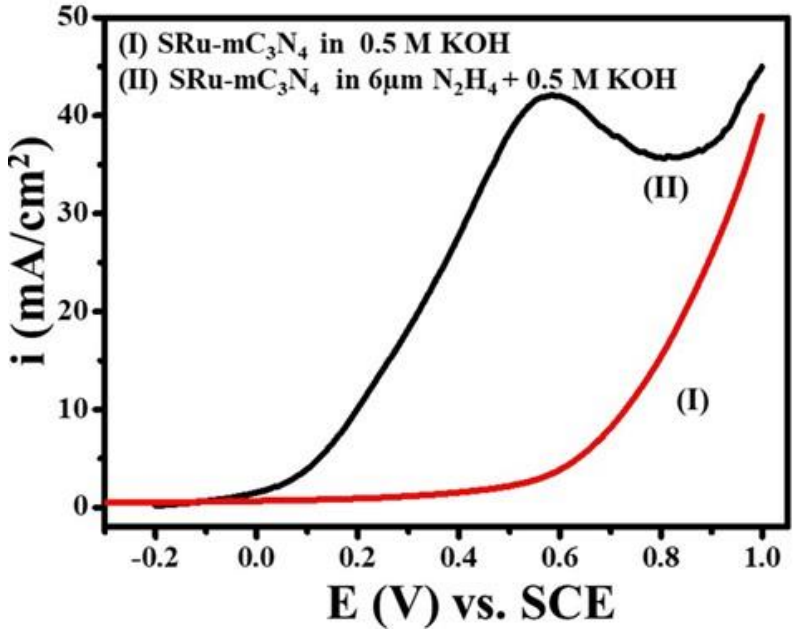

Figure S3. Superimposed linear sweep voltammetry (LSV) for the (I) SRu-mC$_3$N$_4$ in 0.5 M KOH (II) SRu-mC$_3$N$_4$ in 6 µM N_2H_4 + 0.5 M KOH at a scan rate of 50 mV/s.

ii) Chronoamperometric studies

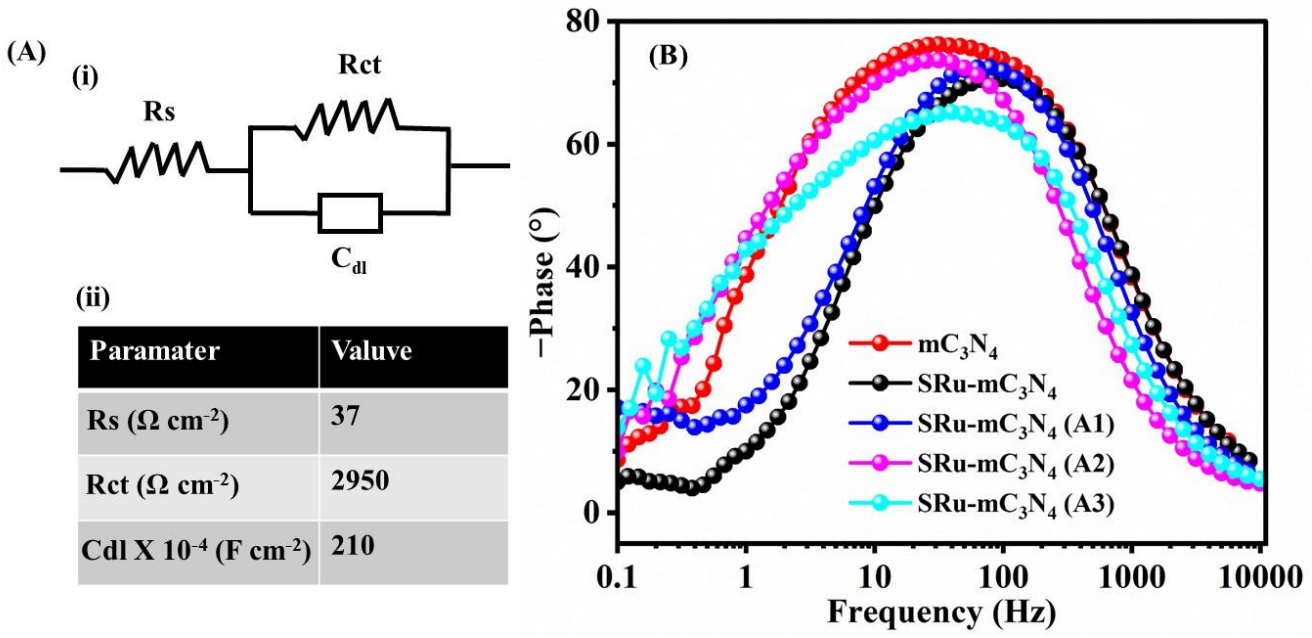

Paramater	Valuve
Rs (Ω cm^{-2})	37
Rct (Ω cm^{-2})	2950
Cdl X 10^{-4} (F cm^{-2})	210

Figure S4. (A) (i) equivalent circuit and (ii) their values for $SRu\text{-}mC_3N_4$, (B) Bode plot calculated by using EIS data of different electrocatalysts in 6μM N_2H_4 + 0.5 M KOH.

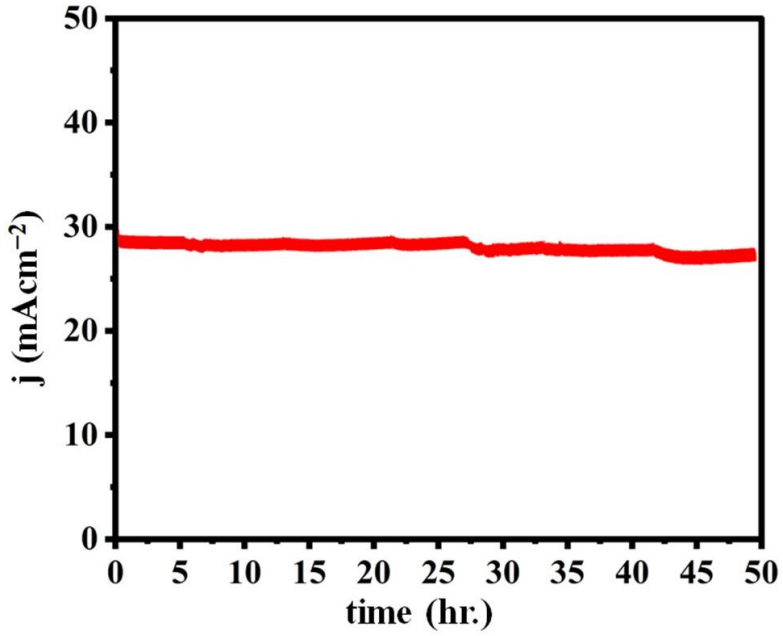

Figure S5. Chronoamperometric studies of $SRu\text{-}mC_3N_4$ in 6 μM N_2H_4 + 0.5 M KOH at an applied potential of 1.3 V vs. RHE (based on obtained current density of 20 mA/cm^2).

S-5) HR-TEM images and Raman spectra of recovered $SRu\text{-}mC_3N_4$ catalyst after electrocatalytic hydrazine oxidation

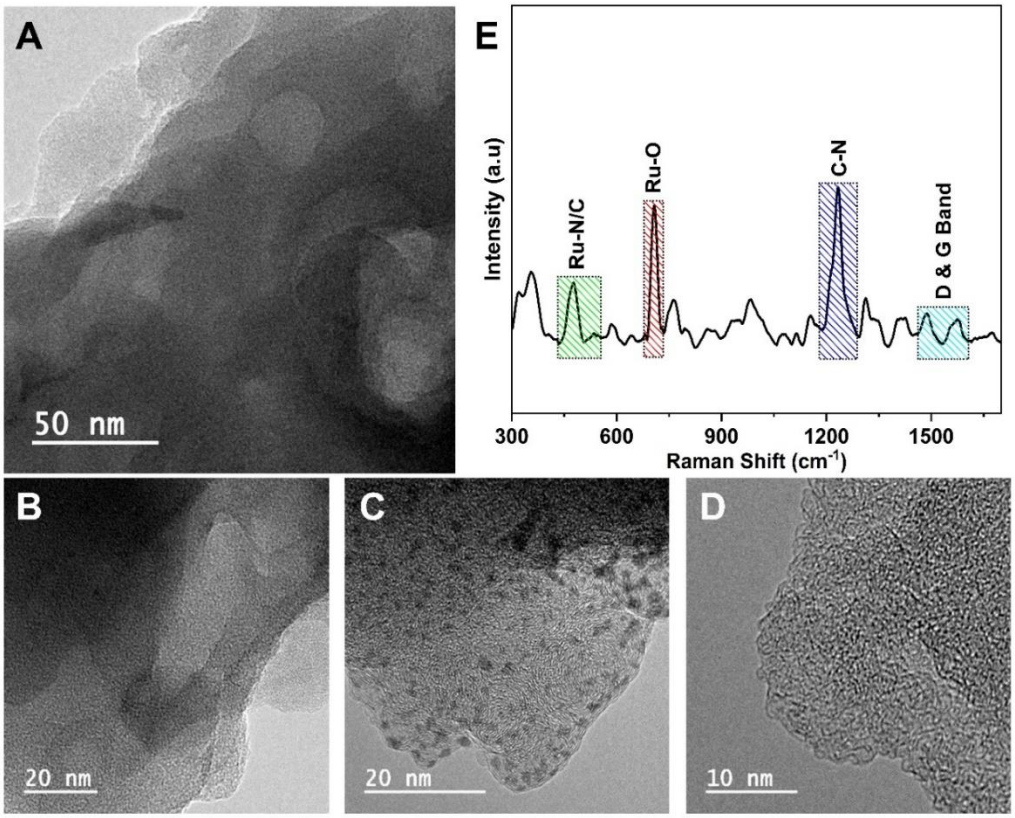

Figure S6. (A-D) HR-TEM images, and (E) Raman spectra of SRu-mC_3N_4 catalyst after electrocatalytic hydrazine oxidation reaction study.

S-6) Calculation for enhancement factor

We determined the electrocatalyst's enhancement factor (EF) at a fixed voltage. SRu-mC_3N_4 is a more effective electrocatalyst than bare GCE, m-C_3N_4, SRu-mC_3N_4 (A1), SRu-mC_3N_4 (A3), and SRu-mC_3N_4 (A2) in a 6 μM N_2H_4 + 0.5 M KOH solution, according to the electrocatalytic activity given in Table 1 based on enhancing factor (EF). The enhancement factor (EF) of SRu-mC_3N_4 is higher (2258) than that of m-C_3N_4 (376), SRu-mC_3N_4 (A1; 617), SRu-mC_3N_4 (A3; 386) and SRu-mC_3N_4 (A2; 364) in 6 μM N_2H_4 + 0.5 M KOH.

$$\textbf{\textit{Enhancement Factor}}\ (\textbf{\textit{EF}}) = \frac{currrent\ density\ of\ electrocatalyst}{Current\ density\ of\ bare\ GCE} \times 100$$

Table S1. Electrochemical performance of previously reported HzOR systems from the literature.

Sr. No.	Electrocatalyst	Electrolyte KOH/N_2H_4	10 mA/cm² (V vs. RHE)	Stability (h)	Reference
1	Ag NPs	0.5 M /0.5 mL	1.57	-	[40]
	Ag@C60		1.21	-	
2	Au-TiO_2	0.1 M / 3 mM	1.18	-	[41]
3	$(Cu_{0.9}Pd_{0.1})O$	0.1 M /10 mM	1.32	0.5	[42]
4	Ni@Pd-Ni alloy NAs	1 M/20 mM	0.94	0.35	[43]
5	MoCx-NC	0.1 M/0.02 M	-	0.78	[44]
6	PdSn/MWCNT	1 M/0.5 M	1.15		[45]

7	Concave TOH Au NCs	0.1 M /10 mM	1.32	10	[46]
8	$Rh/NiFe_{-5.4.}$	1 M/0.2 M	1.38	5.5	[47]
9	$Ru_1/mono\text{-}NiFe_{-0.3}$	1 M/0.2 M	1.34	-	[48]
10	**SRu-mC_3N_4**	**0.5 M /6 μM**	**1.19**	**50**	**This Work**

References

40. Narwade, S.S.; Mulik, B.B.; Mali, S.M.; Sathe, B.R. Silver Nanoparticles Sensitized C60(Ag@C60) as Efficient Electrocatalysts for Hydrazine Oxidation: Implication for Hydrogen Generation Reaction. *Appl. Surf. Sci.* **2017**, *396*, 939–944, doi:10.1016/j.apsusc.2016.11.065.
41. Roy, N.; Bhunia, K.; Terashima, C.; Fujishima, A.; Pradhan, D. Citrate-Capped Hybrid Au-TiO_2 Nanomaterial for Facile and Enhanced Electrochemical Hydrazine Oxidation. *ACS Omega* **2017**, *2*, 1215–1221, doi:10.1021/acsomega.6b00566.
42. Zhang, X.; Shi, S.; Yin, H. CuPd Alloy Oxide Nanobelts as Electrocatalyst Towards Hydrazine Oxidation. *ChemElectroChem* **2019**, *6*, 1514–1519, doi:10.1002/celc.201900148.
43. Du, M.; Sun, H.; Li, J.; Ye, X.; Yue, F.; Yang, J.; Liu, Y.; Guo, F. Integrative Ni@Pd-Ni Alloy Nanowire Array Electrocatalysts Boost Hydrazine Oxidation Kinetics. *ChemElectroChem* **2019**, *6*, 5581–5587, doi:10.1002/celc.201901303.
44. Deng, J.; Li, X.; Imhanria, S.; Chen, K.; Deng, X.; Wang, W. Molybdenum Carbide-Nitrogen Doped Carbon Composites as Effective Non-Precious Electrocatalyst for Direct Hydrazine Fuel Cell. *Electrochim. Acta* **2021**, *384*, 138417, doi:10.1016/j.electacta.2021.138417.
45. Er, O.F.; Cavak, A.; Aldemir, A.; Kivrak, H. Hydrazine Electrooxidation Activities of Novel Carbon Nanotube Supported Tin Modified Palladium Nanocatalysts. *Surfaces and Interfaces* **2022**, *28*, 101680, doi:10.1016/j.surfin.2021.101680.
46. Liu, F.; Jiang, X.; Wang, H.-H.; Chen, C.; Yang, Y.-H.; Sheng, T.; Wei, Y.-S.; Zhao, X.-S.; Wei, L. Boosting Electrocatalytic Hydrazine Oxidation Reaction on High-Index Faceted Au Concave Trioctahedral Nanocrystals. *ACS Sustain. Chem. Eng.* **2022**, *10*, 696–702, doi:10.1021/acssuschemeng.1c07700.
47. Liu, G.; Wang, Z.; Shen, T.; Zheng, X.; Zhao, Y.; Song, Y.-F. Atomically Dispersed Rh-Doped NiFe Layered Double Hydroxides: Precise Location of Rh and Promoting Hydrazine Electrooxidation Properties. *Nanoscale* **2021**, *13*, 1869–1874, doi:10.1039/D0NR07157A.
48. Wang, Z.; Xu, S.-M.; Xu, Y.; Tan, L.; Wang, X.; Zhao, Y.; Duan, H.; Song, Y.-F. Single Ru Atoms with Precise Coordination on a Monolayer Layered Double Hydroxide for Efficient Electrooxidation Catalysis. *Chem. Sci.* **2019**, *10*, 378–384, doi:10.1039/C8SC04480E.